Potential Improvement in Photo Reduction of Towards Cr(VI) Species from Aqueous Solutions onto a Heterogeneous Na-Clay/Fe_2O_3 Catalyst

Yasmine, Bouchemaa; Djamel, Nibou*+; Samira, Amokrane

Laboratory of Materials Technology, University of Science and Technology Houari Boumediene, B.P. 32, El-Alia, Bab-Ezzouar, Algiers, ALGERIA

ABSTRACT: *Clays in the soils are a natural barrier against pollution. A representative sample of clay (illite) from Algeria is collected and analyzed by XRD. The results show that this sample is illite containing calcite and quartz as impurities. We also analyzed the clay by SEM, EDS, and BET, and modified it by chemical treatment with NaCl in order to increase its specific surface area with the insertion of Na^+ cations into the inter-foliar space. The study of Cr(VI) ions adsorption onto Na-Clay was performed. The influence of Cr(VI) initial concentration, pH of the solution, temperature, and solid/liquid ratio was studied. Among the tested models, the equilibrium data are well-fitted by the Langmuir isotherm. The maximum Cr(VI) adsorption rate was 44% at 25°C with limited capacity adsorption of 10 mg/g. The adsorption kinetic is best described by the pseudo-second-order model. The Cr(VI) ions reduction onto* Na-Clay/Fe_2O_3 *and the effect of the same parameters were also performed. The maximum reduction (98%) was reached at pH = 2, T = 25°C, [Cr(VI)] = 50 mg/L, and S/L = 1 mg/mL. It was found that the reaction follows the pseudo-first-order rationalized well by the Langmuir-Hinshelwood (LH) model. The evaluation of the thermodynamic parameters (ΔG°, ΔH°, and ΔS°) revealed that chromium (VI) adsorption and reduction were endothermic and exothermic respectively.*

KEYWORDS: *Adsorption; Photo-catalysis; Na-Clay/Fe_2O_3; Cr (VI) ions; Reduction; Kinetic study.*

INTRODUCTION

Pollution of water and soil is a source of environmental degradation caused by discharges of toxic heavy metals generated by industrial activities which are increasingly becoming the focus of government and citizen concern around the globe [1,2]. Among the heavy metals include chromium which is a highly active and toxic metal with a degree of oxidation that varies from 0 to +6, the more stable is Cr (III). Unlike the Cr (III) complex of chromium in its form of valence VI is highly toxic to its oxidizing power and high mobility in an aqueous environment [3,4]. It is a result of various industries such as the chemical industry, the manufacture of dyes and coloring agents for ceramics, and the galvanization of metals [5-7]. It is therefore essential to eliminate totally the Cr (VI) ions present in industrial effluents or reduce their amount below permissible thresholds defined by international standards, this threshold is fixed

** To whom correspondence should be addressed.*
+ E-mail: dnibou@Yahoo.fr
1021-9986/2022/5/1561-1572 12/$/6.02

at 0.05 mg/L. Many techniques and elimination methods are developed as electrolysis, ion exchange, and adsorption [8-10]. At this level, photocatalysis has shown promise by means of research that have lot progressed in recent years, research has turned towards the destruction of pollutants by the action of semiconducting metal oxides in an aqueous medium [11-13]. These treatment methods to this day are expensive and not always effective using synthetic adsorbents such as zeolites, resins, and organic extractors[13-22]. For this, it is desirable to use and exploit adsorbents available in nature as mineral clays [23]. On the other hand, many adsorbents are currently used to reduce chromium in aqueous solutions such as zeolites, active carbon, and clays [10-13]. The clays have an enormous interest as adsorbents and are effective for removing heavy metals. The interest in the use of clays as adsorbents are justified by their abundance in nature, the importance of surfaces that develop, the presence of electrical charges on the surface, and especially the tradability of inter foliar cations [24].

The insertion of semiconducting oxides in clays is poorly studied despite its importance in water treatment and photocatalysis coupled with the absorbing property of clays and photo reduction of semiconductors for the reason of a better result. In this context, the present work aims at the preparation of an Algerian Clay modified by chemical treatment with NaCl (Na-Clay) and a heterogeneous catalyst (Na-Clay/Fe_2O_3) based on a semiconductor oxide Fe_2O_3 impregnated onto Na-Clay. The samples are firstly characterized by some techniques such as X-Ray Diffraction (XRD), Scanning Electron Microscopy (SEM), Energy Dispersive Spectroscopy (EDS), and finally valorized in the adsorption and photoreduction of Cr(VI) ions in solar irradiation.

EXPERIMENTAL SECTION

Clay preparation

The exchange technique was used to activate an Algerian clay (origin Hammam Boughrara (Maghnia) which is located in the North-West of Algeria) with NaCl (99 %, Merck) according to the following protocol: 15 g of the clay was added to 300 mL of NaCl solution (1M), the mixture is magnetically stirred (4h) at room temperature after which it is dried in an air oven at 65°C overnight. The powder (Na-Clay) thus obtained is grounded to a fine powder ready for the adsorption of chromium (VI) ion. In addition, a heterogeneous catalyst (Na-Clay/Fe_2O_3) was prepared by mixing Na-Clay and Fe2O3 synthesized from $Fe(NO_3)9H_2O$ (98 %, Merck) by hydrothermal method. 12.64g of $Fe(NO_3)9H_2O$ are dispersed in 10 mL of distilled water and then added to 10 g of clay. The mixture is left under stirring for 2 h at room temperature. Then the mixture is heated in the presence of concentrated nitric acid. The resulting mixture is heated to 100 °C to remove water and then to 300 °C to denitrify it. The powder thus obtained is ground for homogenization and then calcined in an oven at 450 °C for 6 hours to obtain the Hematite pure phase.

Characterization

The sample of clay was characterized by X-ray diffraction (Panalytical/expert-pro, using Cu K_α radiation). The surface morphology was observed with a Scanning Electronic Microscope (SEM, Joel JSM 6360) equipped with an Energy Dispersive Spectrometer (EDS) for chemical analysis. The surface-specific area is determined by the BET method using the 2000E instrument software.

Adsorption experiments

The adsorption tests are done in a double jacket batch reactor opened to air. The chromate solutions (50-200 mg/L) are prepared by dilution from a stock solution (1000 mg/L) of $K_2Cr_2O_7$ (99 %, Merck). The reactor was filled with 100 mL of Cr(VI) solution and maintained under moderate agitation (300 rpm) by means of a magnetic stirrer. The dispersion was filtered on a Wattman filter (0.2 µm porosity) and centrifuged. The remaining solution was analyzed by an OPTIZEN1220-type UV-Visible spectrometry device after complexation of Cr^{6+} using diphenylcarbazide reagent (99 %, Merck) at 540 nm according to the standard colorimetric method. The latter consists of mixing 1mL of Cr(VI) solution with 1,5diphenylcarbazide in an acidic medium and after 10 min purplish pink complex forms and is analyzed using a visible UV-Visible [4]. A linear plot was obtained showing the application of the Beer-Lambert law within the concentration range studied.

The removal yield of Cr(VI) is calculated from the relation:

$$(\%)\,\text{Removal of Cr(VI)} = 100\frac{(C0 - Ce)}{C0} \qquad (1)$$

Table 1: The linear form and plot of Langmuir and Freundlich models [25].

Models	Linear form	Plot
Langmuir	$\frac{Ce}{Qe} = \frac{1}{bQmax} + \frac{1}{Qmax}Ce$	$\frac{Ce}{Qe}$ Vs Ce
Freundlich	$\ln Qe = \ln Kf + \frac{1}{n}\ln Ce$	ln Qe Vs ln Ce

Table 2: Pseudo first order and pseudo-second order equations[27].

Models	Equation
Pseudo first order	$\frac{1}{Qt} = \frac{K}{Qe \times t} + \frac{1}{Qe}$
Pseudo second order	$\frac{t}{Qt} = \frac{1}{KsQmax^2} + \frac{1}{Qmax}$ t

where C_0 and C_e are the initial and the equilibrium concentration of the Cr(VI) in the solution respectively.

Isotherm model

In order to describe the removal mechanism of Cr(VI) from water onto activated clay. Two isotherm models (Freundlich and Langmuir isotherm models) were applied to establish the relationship between the amount of Cr(VI) ion adsorbed by activated clay and their equilibrium concentration in aqueous solutions [25-26]. The linear form and the plot of each model were illustrated in Table 1 Where b, Q_{max}, $K_{f,}$ and n are Langmuir constants related to the free energy of adsorption (L/mg), the maximum adsorption capacity (mg/g), Freundlich constant indicative of the relative adsorption capacity of the adsorbent and Freundlich constant indicative of the intensity of the adsorption respectively [25].

Kinetic

The kinetic study was done by the models illustrated in Table 2 [27] where Q_{max} and Q_t are the maximum amounts of metal ion adsorbed per unit mass of the adsorbent (mg/g) and at time t respectively, K and K_s are the first order rate constant (min^{-1}), and the pseudo-second-order kinetic rate constant (g/mg.min).

Thermodynamics

The thermodynamic parameters were evaluated to confirm the nature of the adsorption and the inherent energetic changes involved during Cr(VI) adsorption. Standard enthalpy (ΔH°), free energy (ΔG°), and entropy change (ΔS°) were calculated to determine the thermodynamic feasibility and the spontaneous nature of the process. Therefore, these were determined using the following equations [28]:

$$\Delta G^\circ = -RT \ln Kc \quad (2)$$

$$\Delta G^\circ = \Delta H^\circ - T\Delta S^\circ \quad (3)$$

$$\ln Kc = -\frac{\Delta H^\circ}{RT} + \frac{\Delta S^\circ}{R} \quad (4)$$

where Kc is the equilibrium constant ($Kc = \frac{(C0-Ce)}{Ce}$), R is the universal gas constant (8.314 J/K mol) and T is the absolute temperature (K). The plot of lnKc versus 1/T yields a straight line from which ΔH° and ΔS° are obtained [28].

RESULTS AND DISCUSSION

Characterization

Fig1. shows the XRD pattern of the clay and clay/Na^+. The illite is a major phase and the main characteristic peaks:(2θ: 17.6°; 19.8; 20.9°; 23.8°; 27.7°; 29.7°; 36.6°; 42.4°; 46°; 54;8°) are observed in Fig.1a. Other phases are also present like the kaolinite (2θ: 19.8°; 34.9°; 37°; 73°), the quartz (2θ: 26.5°; 39.5°; 42.8°; 50.1°; 60.1°; 69°), the calcite (2θ: 29.5°; 49.5°) and the Fe_2O_3 (2θ: 33.16°; 35.64° with very short intensity peaks). A new peak (2θ: 8.9°) characteristic of the phase illite/montmorillonite (I/M) is also observed in Fig.1a.

Fig.1b shows the X-ray diffraction pattern of the heterogeneous catalyst Na-Clay/Fe_2O_3. All peaks attributed to Na-Clay are present in the pattern with those of Fe_2O_3 phase known as Hematite [8, 12, 29]. The increase in the intensity of the Fe_2O_3 peaks confirms its incorporation in the structure of Na-Clay. The inter-reticular distances and diffraction angles of Fe_2O_3 present in the new heterogeneous catalyst are regrouped in Table 3.

Table 3: Main inter reticular distances and diffraction angles of hematite phase Fe_2O_3 .

2θ (°)	12.27	19.78	34.85	37.73	38.35	45.52	51.11	62.35
d (Å)	7.205	4.484	2.571	2.381	2.344	1.990	1.785	1.480
(hkl)	001	020	-201	003	-202	-203	004	060

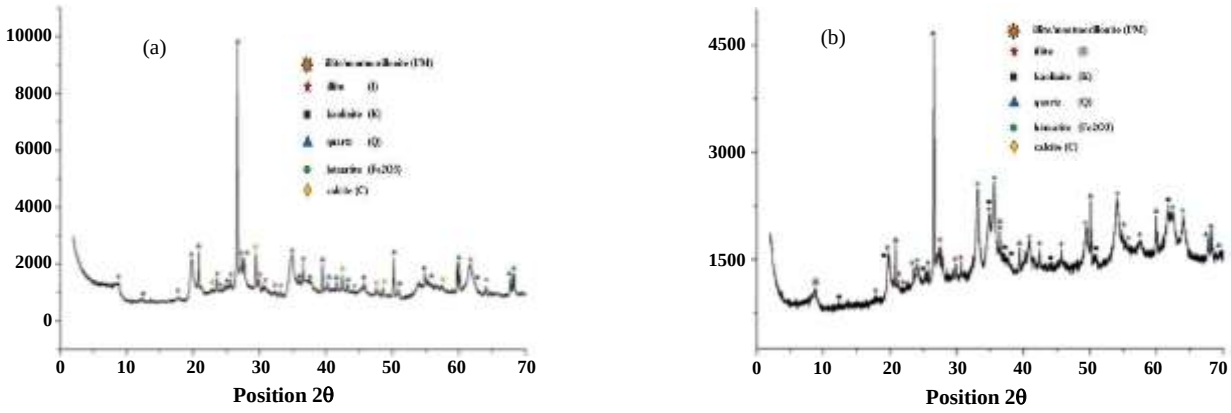

Fig.1: a) X-ray diffraction pattern of Na-Clay. b) X-ray diffraction pattern of heterogeneous catalyst Na-Clay/Fe_2O_3)

The SEM micrographs (Fig.2) show that the rough clay, Na-Clay, and Na-Clay/Fe_2O_3 consist mainly of grains arranged as sheets identifying with the typical structure of clays. Fig.2 (b) and Fig.2 (C) show that the surface of the clay matrix was covered with NaCl and Fe_2O_3 particles.

The results of the EDS spectra confirm the presence of the main elements' mineralogical composition in the clay samples. From the results of Fig.2 (b), the Na is detected in the framework due to the treatment of rough clay with NaCl. The increase of Fe in the chemical composition of Na-Clay is also due to the presence of hematite Fe_2O_3 as shown in Fig.2 (c).

The specific surface areas of Na-Clay and Na-Clay/Fe_2O_3 determined from BET measurements average 134.7 and 149.5 m²/g respectively with a high porosity which is much large compared to that of rough clay (13.18 m²/g).

Adsorption experiment

Effect of chemical treatment and chromate concentration on the adsorption process

A comparative study of the adsorption behavior of chromium (VI) ions by the rough clay and activated clay (Na-Clay) was realized with a concentration 50 mg/L. The results in Fig.3 show then the chemical treatment of the rough clay with NaCl gives it the best performance. The treatment of the clay by NaCl is responsible for the increase of the specific surface from 13.18 to 134.7 m²/g

The effect of Cr(VI) initial concentration on the adsorption process was also investigated in the ranges of 10-200 mg/L, while the rest of the parameters were kept the same as optimized in the previous experiments. The percentage of chromium adsorption increased with decreasing the initial chromium concentration. This strong adsorption for low initial chromium concentration might be explained by the active sites available on the adsorbent similar results have been reported in the literature [30-31].

According to Fig.3, we noticed also that the optimum contact time can be deduced. The adsorption efficiency increases and over 22 and 38 % of the adsorbed Cr(VI) ions occurred within 60 to 70 min using rough clay and Na-Clay respectively. Beyond 80 min, the adsorption rate was observed to be kept constant and we consider that the adsorption equilibrium can be established and 80 min was selected as the contact time.

Effect of temperature on the adsorption process

The effect of temperature on the adsorption of chromium (VI) ions efficiency was investigated in the range of 25 to 50°C (Fig.4). The percentage of adsorption increased to 72 % with increasing temperature to 50°C indicating that the process is endothermic.

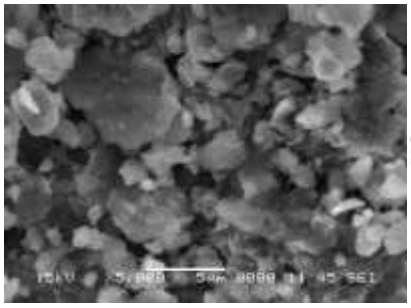

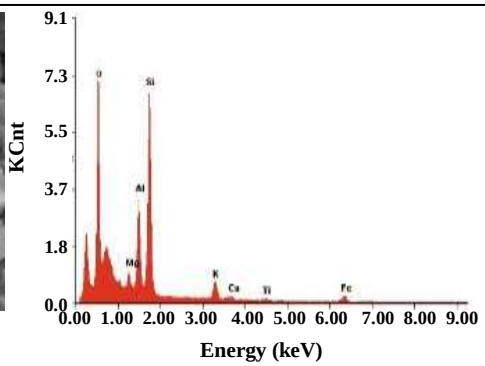

Elem	Wt%	At%
O K	32.65	42.85
MgK	03.31	04.17
AlK	18.81	21.34
SiK	53.88	58.71
KK	09.06	07.09
CaK	01.68	01.28
FeK	11.77	06.45

(a)

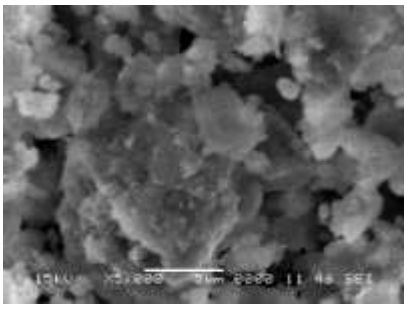

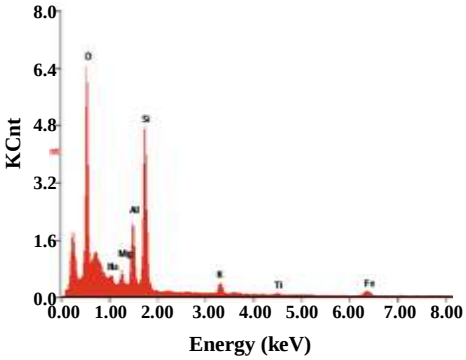

Elem	Wt%	At%
OK	29.43	39.53
NaK	01.78	02.33
MgK	03.62	04.49
AlK	18.20	20.36
SiK	55.53	59.70
KK	07.30	05.64
FeK	12.13	06.56

(b)

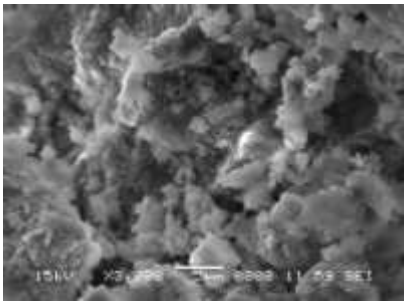

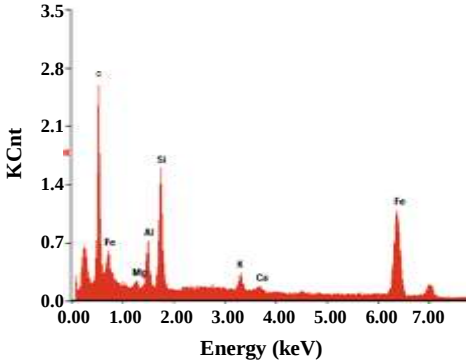

Elem	Wt%	At%
OK	23.42	33.62
MgK	01.05	01.92
AlK	06.02	09.95
SiK	15.77	25.04
KK	03.21	03.66
CaK	01.26	01.40
FeK	72.69	58.03

(c)

Fig. 2: SEM micrographs, EDS spectra, and chemical compositions of (a) rough Clay, (b) Na-Clay, and (c) Na-Clay/Fe_2O_3.

As is reported in the literature [32], an increase in temperature is known to increase the diffusion rate of the adsorbate ions across the external boundary layer and in the internal pores of the adsorbent particles as a result of the decreased viscosity of the solution.

Isotherm study

The Langmuir and Freundlich model parameters of the sorption data are given in Table 4. The results show that Langmuir model describes the adsorption data with R2 value 0.983 according to the saturated monolayer adsorption. The obtained maximum adsorption capacity value is 10 mg/g. On the other hand, the equilibrium data were analyzed using Freundlich isotherm model with R2 value of 0.918. Generally, n is a dimensionless parameter and presents the heterogeneity factor [26]. Values of n > 1 represent favorable adsorption conditions [25]. Obtained value n of 1.90 represents a favorable adsorption process.

Table 4: The parameter's value of Langmuir and Freundlich models.

Langmuir				Freunlich		
Q_{max} (mg.g^{1})	B (L.mg^{1})	R_L	R^2	K_f (L.g^{1})	n	R^2
10	0.027	0.425	0.983	0.7	1.90	0.918

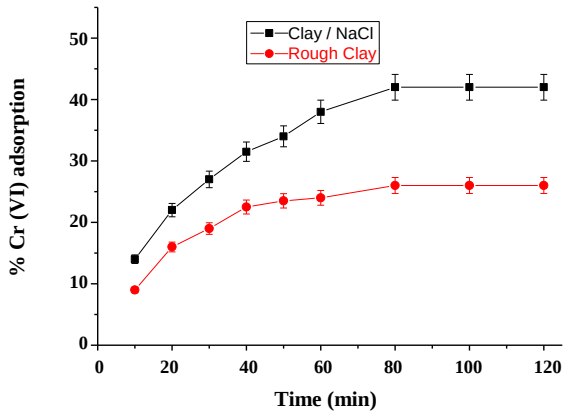

Fig. 3: Effect of chemical treatment on clay.

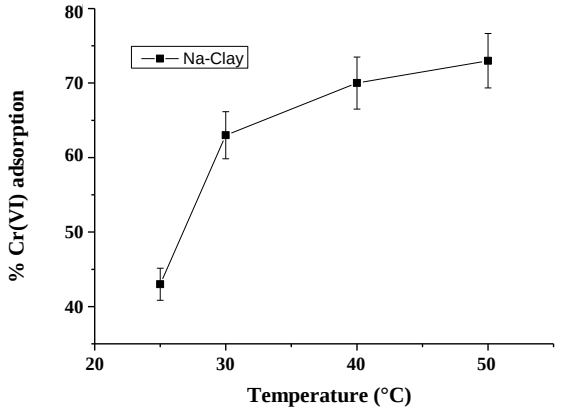

Fig. 4: Effect of Cr(VI) adsorption versus temperature (C_0 = 50mg/L, pH = 2, S/L = 1mg/mL).

This isotherm does not predict any saturation of the inter foliar space of Na-Clay by Cr(VI) ions; thus infinite surface coverage is predicted and indicates multilayer adsorption on the surface. Comparing the R2 values of the two isotherm models, it seems that Langmuir model has better performance than Freundlich for representing the equilibrium data.

The value of separation factor RL, a fundamental characteristic of Langmuir isotherm model ($R_L = 1/(1 + bC_0)$), shows that the adsorption of chromium (VI) onto Na-Clay was more favorable. As reported in the literature [10, 32], The values of R_L indicated the type of Langmuir isotherm to be favorable ($0<R_L<1$), unfavorable ($R_L > 1$), linear ($R_L=1$), or irreversible ($R_L = 0$).

Kinetic adsorption study

The results presented in Table 5 show that the low correlation coefficient values obtained for the pseudo-first-order models indicate that the adsorption of Cr(VI) ions did not follow the pseudo-first-order kinetic. The insufficiency of the first-order model to fit the kinetics data can be explained by the limitations of the boundary layer controlling the adsorption process [20,21].

On the other hand, the variation of t/Qt as a function of t is linear as clearly shown in Fig.5 and the regression analysis gives values ($R^2 > 0.979$) which indicated that the adsorption system studied belongs to the pseudo-second-order kinetic model.

The values of calculated and experimental Q_{exp} were very close which also concluded that the adsorption of Cr(VI) ions onto Na-Clay could be better explained by pseudo-second-order model than others.

Thermodynamic adsorption study

The thermodynamic adsorption parameters are given in Table 6. As can be seen in the ΔG° values are negative for all temperatures, indicating that Cr(VI) ions adsorbed spontaneously onto activated clay and that the system does not gain energy from an external source. The positive value of ΔH° further confirms the endothermic nature of chromium adsorption, while positive entropy (ΔS°) indicates the increased randomness with chromium adsorption, probably because the number of desorbed water molecules is larger than that of adsorbed Cr(VI) molecules [26,27].

Photoreduction experiments

One can observe that the treated clay is limited in the adsorption of Cr(VI) ions. The maximum Cr(VI) percentage reached a value of about 44 % at 25°C with limited capacity adsorption Q_{max} of about 10 mg/g calculated from Langmuir isotherm. The non adsorbed

Table 5: Pseudo first order and second order parameters.

C (mg/L)	Pseudo first order		Pseudo second order	
	K_1	R^2	K_2	R^2
50	0.046	0.917	0.130	0.970
75	0.048	0.882	0.086	0.972
100	0.0483	0.887	0.074	0.985
150	0.032	0.902	0.036	0.939
200	0.052	0.865	0.026	0.913

Table 6: Thermodynamic parameters for the adsorption of Cr(VI) onto Na-Clay at different temperatures.

T (K)	ΔG°(KJ/mol)	ΔH°(KJ/mol)	ΔS°(J/mol K)
298	-12.42		
303	-14.65	39.01	161.57
313	-15.97		
323	-16.73		

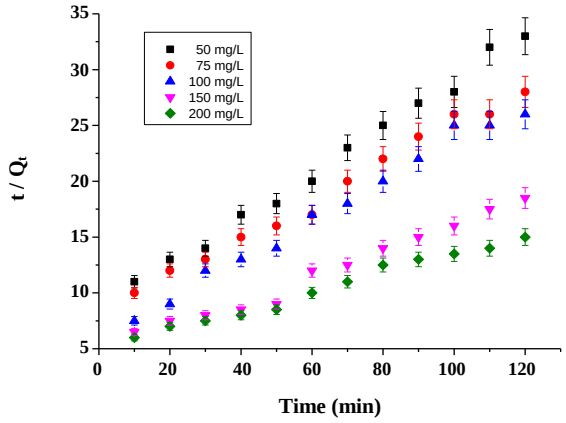

Fig. 5: Pseudo second-order model for the adsorption of Cr(VI) ions by Na-Clay.

Cr(VI) ions in solution were reduced by photocatalysis process to Cr(III) species using the same treated clay with NaCl and doped with Fe_2O_3. The obtained heterogeneous catalyst (Na-Clay/Fe_2O_3) is characterized by semi-conductor properties required in the photoreduction reaction. The oxide Fe_2O_3 is a semiconductor necessary in photocatalysis. Its excitation by a maximum light source (hv), gives excited electrons which will pass from the valence band (BV) by creating an oxidation site (h^+ hole) towards the conduction band (BC) by creating a reduction site (electron e^-). Fe_2O_3 is a suitable photocatalyst since it is less expensive with its wide band gap (Eg) and requires an excitation in the UV region. Fe_2O_3 oxide was used effectively in previous works [8, 12, 33].

The photoreduction reaction occurred in presence of oxalic acid ($C_2H_2O_4$) known with its distinct chemical characteristic to be an energetic reducer as reported by *Sebati et al.* [34]:

$$Fe_2O_3 / Clay + h\upsilon \rightarrow h^+_{VB} + e^-_{CB} \quad (5)$$

$$HCrO_4^- + 7\,H_3O^+ + 3e^- \rightarrow Cr^{3+} + 11\,H_2O \quad (6)$$

$$2H_2O + 2e^- \rightarrow H_2 + 2\,OH^- \quad (7)$$

$$3C_2H_2O_4 + 1/2O_2 + 4h^+ \rightarrow 6CO_2 + H_2O + 4H^+ \quad (8)$$

$$HCrO_4^- + 3/2C_2H_2O_4 + 4\,H_3O^+ \rightarrow 3\,CO_2 + Cr^{3+} + 8\,H_2O \quad (9)$$

where h^+_{VB} is a gap issued to the passage of exited electron from the valence band VB to conduction band CB carrying out a reduction site (e^-_{CB}).

The effect of physical parameters pH, S/L ratio, initial Cr(VI) concentration, and temperature on the photocatalytic activity of heterogeneous catalyst Na-Clay/Fe_2O_3 was studied.

Effect of pH

The pH of the solution is a controlling parameter that strongly affects the reduction of Cr(VI) ions onto

Na-Clay/Fe_2O_3 surface and interface. The influence of pH on Cr(VI) reduction was investigated over the range from 1 to 6 keeping all other parameters constants (T = 25°C, C_0 = 50 mg/L, S/L = 1 mg/mL and Stirring rate = 250 tr/min). In this range of pHs, several chromium species are present as H_2CrO_4 (pH<1), $HCrO^{4-}$ (1<pH<6) and CrO_4^{2-} (pH > 6) [7,12].

Fig.6 shows that the rate of reduced Cr(VI) ions decreases with increasing pH and the maximum reduction (98%) is reached at pH between 1 and 2. The rate of reduction of 50% is obtained at pH 3 and decreases to 20% until pH 6. In these conditions, the catalyst surface and interface are charged positively and react favorably with $HCrO^-_4$ species making possible the reduction process (Eq. (6)). It is clear that prepared Na-Clay/Fe_2O_3 offers a high specific surface that favors the formation of active sites at acid pHs is probably responsible for chromate binding and thus reduction of catalyst performance.

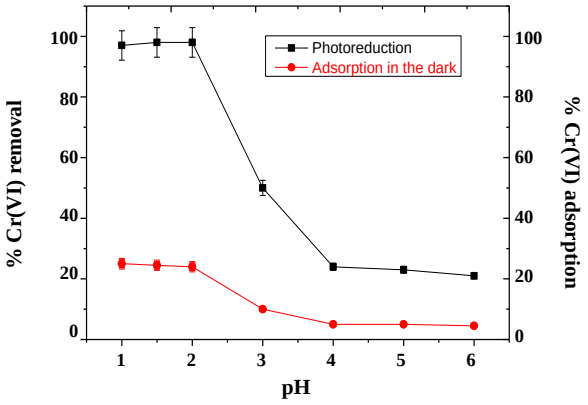

Fig.6: Effect of pH on the adsorption in the dark and the photoreduction of Cr(VI onto Na-Clay/Fe_2O_3 (C_0 = 50 mg/L, S/L = 1 mg/mL, T = 25°C).

Effect of the solid/liquid ratio

The effect of the solid/liquid ratio on the adsorption in the dark and the photoreduction of Cr(VI) onto Na-Clay/Fe_2O_3 is shown in Fig. 7. It can be seen that both percentages of chromium reduction and adsorption increase with increasing of (S/L) ratio. A maximum photoreduction of Cr(VI) ions is obtained at 81% for an (S/L) ratio of about 1 mg/mL. This is due probably to an increase in photocatalytic sites with a high receipt surface for the incident photons. The same phenomenon can be observed in the case of the Cr(VI) ions adsorption process in the dark which occurs with the photo activity similarly [12].

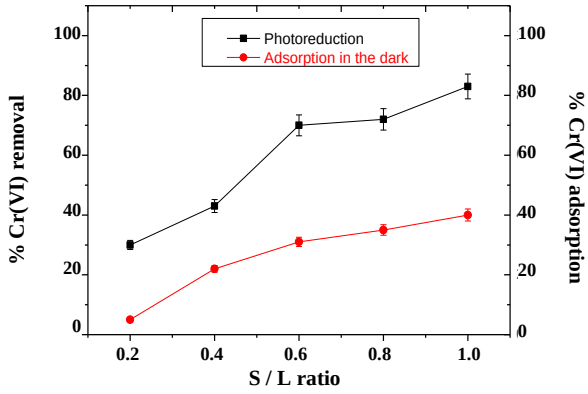

Fig.7: Effect of S/L ratio on the adsorption in the dark and the photoreduction of Cr(VI) onto Na-Clay/Fe_2O_3 (C_0= 50 mg/L, T=25°C, pH= 2).

Effect of the chromate concentration

From Fig.8, it is clear that the rate of reduction of Cr(VI) ions depends on their initial concentration, the evolution varies inversely. The increase of concentration in the solution favors the ionic force, this affects the competition on the active sites of Na-Clay/Fe_2O_3 catalyst reducing the adsorbed amounts in the solution. Elsewhere, The efficiency of catalytic activity depends also on the Cr(VI) initial concentration due probably to the occupation of active sites of Fe_2O_3 by $HCrO_4^-$ trapping the catalyst exciting electrons [33, 35].

The results clearly show that the value of 50 mg/L is optimal in these conditions of adsorption and photoreduction. According to Fig.9, the optimum contact time

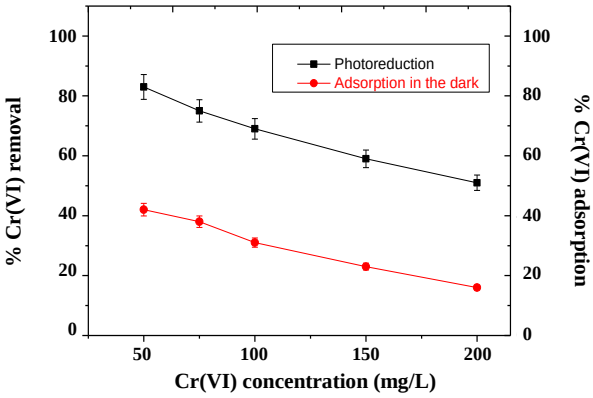

Fig. 8: Effect of initial concentration on the adsorption in the dark and the photoreduction of Cr(VI) onto Na-Clay/Fe_2O_3 (S/L = 1 mg/mL, T = 25°C, pH = 2).

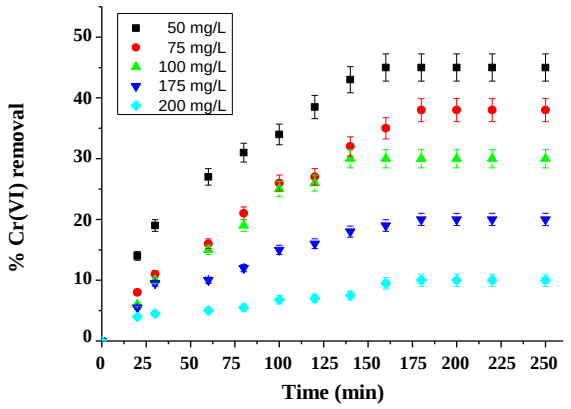

Fig.9. Evolution of % Cr(VI) reduction versus time (pH = 2, S/L = 1 mg/mL, T = 25°C) on Na-Clay/Fe_2O_3 catalyst and at different concentrations.

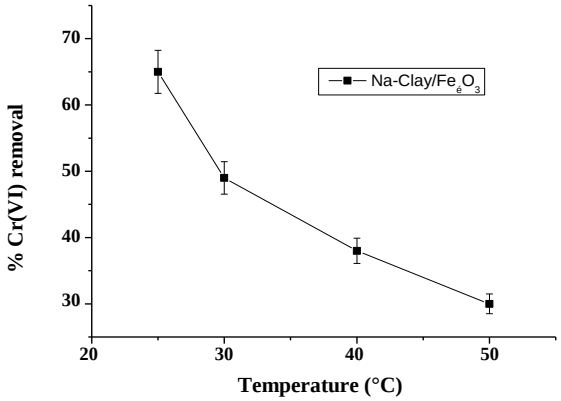

Fig. 10: Effect of Cr(VI) reduction versus temperature (C_0 = 50mg/L, pH = 2, S/L = 1mg/mL).

can be selected after 130 min when the reduction rate was observed to be kept constant at different Cr(VI) ion concentrations.

150 min was chosen as the contact time in these experiments. We notify also that the contact time in reduction of Cr(VI) by photocatalytic reaction (150 min) is longer than the adsorption of these ions (80 min) due to the difference in the mechanism of the two processes [10-12, 18].

Effect of temperature

The effect of temperature on the reduction of chromium (VI) ions efficiency was investigated in the range of 25 to 50°C (Fig.10). The percentage reduction decreased with increasing temperature indicating that the process is exothermic due to the probable recombination of pairs (h^+ / e^-) (Eq. (2)). This affects the competition on the active sites of Na-Clay/Fe_2O_3 catalyst with Cr(VI) species and thus reduces their amounts.

Kinetic adsorption study

Langmuir-Hinshelwood (LH) kinetic model was used to study the rate reaction. This model considers that the adsorption reaction onto the surface of the catalyst occurs with a proportional rate to the production of adsorbed species [11, 13]. It is generally applied to photocatalysis reactions and it is expressed as follows:

$$r = -dC/dt = K_{app} C_0 \quad (10)$$

Where r (min^{-1}) is the apparent initial rate and C_0 is the Cr(VI) concentration. K_{app} is also expressed by:

$$K_{app} = K_r K_s \quad (11)$$

Where K_s(L./mg) is the adsorption equilibrium constant of LH and K_r(mg/(L.min)) is the reaction rate constant.

After integration of Eq. (7), it becomes as follows:

$$Ln(C_0 / C) = K_{app} t \quad (12)$$

The values of $Ln(C_0/C)$ were linearly correlated with t and the plot gives the apparent initial rate K_{app} (Fig.11).

The values of apparent kinetic constants K_{app} are dependent on the initial concentration and are regrouped in Table 7.

The results show that the photocatalysis reaction process follows well the pseudo-first-order kinetic rationalized by Langmuir-Hinshelwood model with coefficient regression values R^2 close to 1. This model is valid for reactions taking place at the solid-liquid interface as in our case. By modifying the LH model by introducing the Langmuir adsorption equilibrium (K_s) and reaction rate (K_r) constants according to the following relation:

$$1/K_{app} = (1/K_s K_r) + C_0 / K_r \quad (13)$$

The plot $1/k_{app}$ as a function of C_0 (Fig.12) gives the values of K_s (0.025 L/mg) and K_r (0.2022 mg/(L.min) respectively.

Table 7: Kinetic parameters of Cr(VI) photo reduction onto Na-Clay/Fe_2O_3.

Concentration (mg/L)	R^2	K_{app} (min^{-1})	$1/K_{app}$	K_r (mg/L.min)	K_s (L/mg)
50	0.998	0.0060	166.66	0.2022	0.025
75	0.994	0.0020	500		
100	0.996	0.0015	666.66		
150	0.998	0.0012	833.33		
200	0.997	0.0010	1000		

Table 8: Thermodynamic parameters for the reduction of Cr(VI) onto Na-Clay/ Fe_2O_3.

	ΔH° (kJ/mol)	ΔS° (J/mol.K)	ΔG° (kJ/mol)			
			298 K	303 K	313 K	323 K
Na-Clay/Fe_2O_3	-42.49	-82.25	-18.33	-17.13	-16.51	-16.05

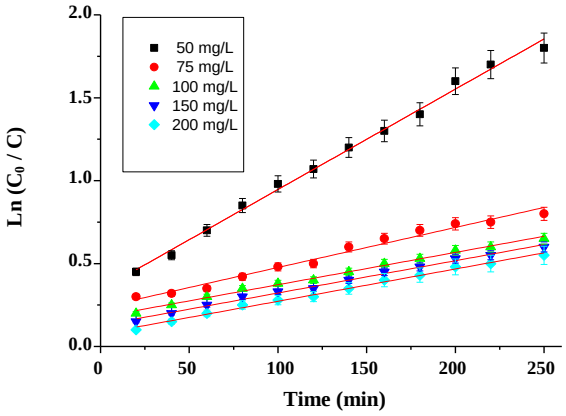

Fig. 11: Kinetic of chromium (VI) photoreduction onto Na-Clay/Fe_2O_3 at different concentrations (pH = 2, S/L = 1 mg/mL, T = 25°C).

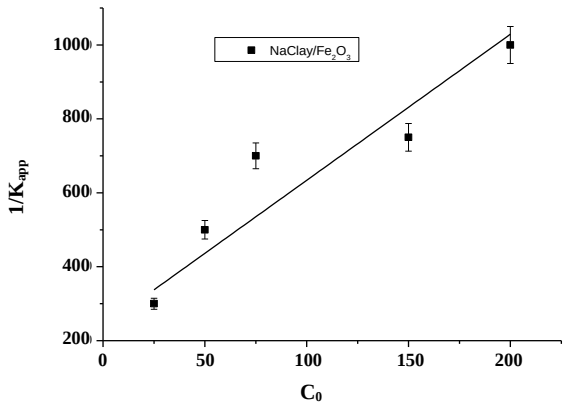

Fig.12. $1/K_{app}$ versus Cr(VI) initial concentration.

The thermodynamic parameters are grouped in Table 8. According to our results, the values obtained for enthalpy (ΔH°), entropy (ΔS°), and free energy (ΔG°) are negative showing that the reaction is exothermic and spontaneous.

CONCLUSIONS

The main purpose of this present study was to test the adsorbing power of a natural and modified clay with regard to the adsorption of Cr(VI) and to optimize our results in the context of their elimination as well as the study of the reducing effect using a heterogeneous catalyst. Indeed, our study demonstrated the limited performance of natural and Na-Clay in the adsorption of Cr (VI) ions (44 %) and the effectiveness of the system Na-Clay/Fe_2O_3 in their reduction to Cr (III) by the photocatalysis process (98%). Langmuir isotherm has a better fitting model indicating the applicability of a monolayer coverage of the Cr(VI) on the surface of Na-Clay adsorbent. It was revealed that the pseudo-second-order kinetic illustrated well the adsorption kinetic and the thermodynamic parameters indicate a spontaneous and endothermic process. The optimized parameters, Cr(VI) concentration (50 mg/L), temperature (25°C), Solid/Liquid ratio (1 mg/mL), and pH (2) were also used in the reduction Cr(VI) ions by photocatalysis reaction. It has been shown that the reduction is favored at low temperatures and the obtained thermodynamic parameters confirm the nature of the exothermic process. The photocatalysis reaction process followed well the pseudo-first-order kinetic established by Langmuir-Hinshelwood model confirming that our reaction took place at the Na-Clay/Fe_2O_3 - liquid interface.

Acknowledgment

Our big gratitude to the General Direction of Scientific Research and Technological Development (GDSRTD) and the Thematic Research Agency in Science and Technology (TRAST) of the Ministry of Higher Education and Scientific Research of the Democratic Republic of Algeria.

Received : May. 13, 2021 ; Accepted : Aug. 30, 2021

[1] Nibou D. and Amokrane S., Mechanism of Cu^{2+} Ions Uptake Process by Synthetic NaA Zeolite from Aqueous Solution: Characterization, Kinetic, Intra-Crystalline Diffusion and Thermodynamic Studies, *J. Molliq.*, **323:** 114642 (2021).

[2] Nibou D. and Amokrane S., Catalytic Performances of Exchanged Y faujasites by Ce^{3+}, La^{3+}, UO_2^{2+}, Co^{2+}, Sr^{2+}, Pb^{2+}, Tl^{+} and NH_4^{+} Cations in Toluene Dismutation Reaction, *Compt. Rend. Chim.*, **13(5)**: 527-537 (2010).

[3] Jamshaid I.M., Cecil F., Khalil A., Munawar I., Mushtaq M., Naeem M.A., Bokhari T.H., Kinetic Study of Cr(III) and Cr(VI) Biosorption Using Rosa Damascena Phytomass: A Rose Waste Biomass, *J. Chem.*, **25**: 2099-20103 (2013)

[4] Aid A., Amokrane S., Nibou D., Mekatel E., Trari M., Hulea V., Modeling Biosorption of Cr (VI) onto Ulva Compressa L. from Aqueous Solutions, *Wat. Sci. Tech.*, **77** (**1**), 60-69 (2018).

[5] Dakiky M., Khamis M., Manassra A., Mereb M., Selective Adsorption of Chromium(VI) in Industrial Wastewater Using Low-Cost Abundantly Available Adsorbents, *Adv. Environ. Res.*, **6:** 533-540 (2002)

[6] Rengaraj S., Joo C.K, kim Y., Yi J., Kinetics of Removal of Chromium from Water and Electronic Process Wastewater by Ion Exchange Resins: 1200 H, 1500 Hand IRN97H, *J. Hazard. Mater.*, **B102**: 257-275 (2003)

[7] Ladjali S., Amokrane S., Mekatel E.H., Nibou D., Adsorption of Cr(VI) on *Stipa tenacissima* L (Alfa): Characteristics, Kinetics and Thermodynamic Studies, Adsorption of Cr(VI) on *Stipa tenacissima* L (Alfa):Characteristics, Kinetics and Thermodynamic Studies, *Sep. Sci. Tech.* , **54 (6)**: 876-887 (2019)

[8] Barquist K., Larsen S.C., Chromate Adsorption on Bifunctional, Magnetic Zeolite Composites, M*icro. Meso. Mater.*, **130**: 197–202 (2010).

[9] Mekatel H., Amokrane S., Benturki A., Nibou D., Treatment of Polluted Aqueous Solutions by Ni^{2+}, Pb^{2+}, Zn^{2+}, Cr^{+6}, Cd^{2+} and Co^{2+} Ions by Ion Exchange Process Using Faujasite Zeolite, *Proc. Eng.*, **33**: 52–57 (2012).

[10] Barkat M., Nibou D., Chegrouche S., Mellah A., Kinetics and Thermodynamics Studies of Chromium (VI) Ions Adsorption onto Activated Carbon from Aqueous Solutions, *Chem. Eng. Proc. Pro. Intens.*, **48(1)**: 38-47 (2009).

[11] Vignesha K., Priyankab R., Rajarajanc M., Suganthia A., Photoreduction of Cr(VI) in Water using Bi_2O_3–ZrO_2 Nanocomposite under Visible Light Irradiation, *Mate. Sci. Eng. B*, **178(2):**149–157 (2013).

[12] Mekatel H., Amokrane S., Bellal B., Trari M., Nibou D., Photocatalytic Reduction of Cr (VI) on Nanosized Fe_2O_3 Supported on Natural Algerian Clay: Characteristics, Kinetic and Thermodynamic Study, *Chem. Eng. J.*, **200:** 611-618 (2012).

[13] Mekatel E.H., Nibou D., Trari M., Amokrane S., Dahdouh N., Removal of Maxilon Red Dye by Adsorption and Photocatalysis: Optimum Conditions, Equilibrium and Kinetic Studies, *Iran. J. Chem. Chem. Eng. (IJCCE)*, **40(1)**: 93-110 (2021).

[14] Zeng Y., Woo H., Lee G., Park J., Adsorption of Cr(VI) on Hexadecylpyridinium Bromide (HDPB) Modified Natural Zeolites, *Micro. Meso. Mater.*, **130**: 83–91 (2010)

[15] Liu S.S., Chen Y.Z., Zhang L.D., Hua G.M., Xu W., Li N., Zhang Y., Enhanced Removal of Trace Cr(VI) Ions from Aqueous Solution by Titanium Oxide –Ag Composite Adsorbents, *J. Hazard. Mater.* **190**: 723-728 (2011)

[16] Venditti F., Ceglie A., Palazzo G., Colafemmina G., Lopez F., Removal of Chromate from Water by a New CTAB-Silica Gelatin Composite, *J. Coll. Inter. Sci.* **310**: 353–361(2007).

[17] Samani M.R., Borghei S.M., Olad A., Chaichi M.J., Influence of Polyaniline Synthesis Conditions on Its Capability for Removal and Recovery of Chromium from Aqueous Solution, *Iran. J. Chem. Chem. Eng. (IJCCE)*, **30 (3):** 97-100 (2011).

[18] Ba S., Ennaciri K., Yaacoubi A., Alagui A., Bacaoui A., Activated Carbon from Olive Wastes as an Adsorbent for Chromium Ions Removal, *Iran. J. Chem. Chem. Eng.*, **37(6):** 107-123 (2018)

[19] Esmaeili A., Ghasemi S., Zamani F., Investigation of Cr(VI) Adsorption by Dried Brown Algae Sargassum Sp. and its Activated Carbon, *Iran. J. Chem. Chem. Eng*., **31(4):** 11-19 (2012)

[20] Aghaie H., Barmaki Z., Seif A., Monajjemi M., Kinetic and Thermodynamic Study of Chromium Picolinate Removing from Aqueous Solution onto fhe Functionalized Multi-Walled Carbonnanotubes, *Iran. J. Chem. Chem. Eng. (IJCCE)*, **40(3)**: 765-779 (2021).

[21] Krobba, A., Nibou, D., Amokrane, S., Mekatel, H., Adsorption of Copper (II) onto Molecular Sieves NaY, *Desal. Wat. Treat.*, **37**: 1–7 (2012).

[22] Aid A., Amokrane S., Nibou D., Mekatel H., Removal of Cr^{6+}, Co^{2+} and Ni^{2+} Ions from Aqueous Solutions by Algerian Enteromorpha Compressa (L.) Biomass, *World Academy of Science, Engineering and Technology, Inter. J. Ecol. Eng.*, **11:** 11 (2017).

[23] Zeng Y., Woo H., Lee G., Park J., Removal of Chromate From Water Using Surfactant Modified Pohang Clinoptilolite and Haruna Chabazite, *Desalination* **257**: 102–109 (2010)

[24] Houhoune F., Nibou D., Chegrouche S., Menacer S., Behaviour of Modified Hexadecyltrimethylammonium Bromide Bentonite Toward Uranium Species, *J. Env. Chem. Eng.* **4 (3)**: 3459-3467 (2016).

[25] Benmessaoud A. Nibou D., Mekatel E.H., Amokrane S., A comparative Study of The Linear and Non-Linear Methods for Determination of the Optimum Equilibrium Isotherm for Adsorption of Pb^{2+} Ions onto Algerian Treated Clay, *Iran. J. Chem. Chem. Eng. (IJCCE)*, **39(4)**: 153-171 (2020).

[26] Nibou D., Mekatel H., Amokrane S., Barkat M., Trari M., Adsorption of Zn^{2+} Ions onto NaA and NaX Zeolites: Kinetic, Equilibrium and Thermodynamic Studies, *J. Hazard. Mater.*, **173**: 637-646 (2010).

[27] Barkat M., Nibou D., Amokrane S., Chegrouche S., Mellah A., Uranium (VI) Adsorption on Synthesized 4A and P1 Zeolites: Equilibrium, Kinetic, and Thermodynamic Studies, *Com. Rend. Chim.*, **18 (3)**: 261-269 (2015).

[28] Ferhat D., Nibou D., Mekatel E.H., Amokrane S., Adsorption of Ni^{2+} Ions onto NaX and NaY Zeolites: Equilibrium, Kinetic, Intra Crystalline Diffusion and Thermodynamic Studies, *Iran. J. Chem. Chem. Eng. (IJCCE)*, **38(6)** : 63-81 (2019).

[29] Nibou D., Amokrane S., Lebaili N., Use of NaX Porous Materials in the Recovery of Iron Ions, *Desalination* **250(1)**: 459-462 (2010).

[30] Leyva-Ramos R., Jacobo-Azuara A., Diaz-Flores P.E., Guerrero-Coronado R.M., Mendoza-Barron J., Berber-Mendoza M.S., Adsorption of Chromium(VI) from an Aqueous Solution on a Surfactant-Modified Zeolites, *Coll. Surf. A: Phy. Eng. Aspects*, **330**: 35–41(2008)

[31] Mekatel E.H., Amokrane S., Aid A., Nibou D., Trari M., Adsorption of Methyl Orange on Nanoparticles of a Synthetic Zeolite NaA/CuO, *Com. Rend. Chim.* **18(3)**: 336-344 (2015).

[32] Houhoune F., Djamel N., Samira A., Mahfoud B., Modelling and Adsorption Studies of Removal Uranium (VI) Ions on Synthesised Zeolite NaY, *Des. Wat. Treat.*, **51(28-30)**: 5583-5591(2013)

[33] Haddad D., Mellah A., Nibou D., Khemaissia S., Promising Enhancement in The Removal of Uranium Ions by Surface-Modified Activated Carbons: Kinetic and Equilibrium Studies, *J. Environ. Eng.*, **144(5)**: 04018027 (2018)

[34] Sebati F., Nibou D., Amokrane S., Comparative Study of the Adsorption and Photo-Reduction of Hexavalent Chromium onto $AlPO_4$-11 and SAPO-31 Substituted Fe_2O_3 from Aqueous Solutions: Synthesis, Characterization, Kinetic and Thermodynamic Studies, *Sep. Sci. Tech.*, **56(12)**: 2011-2025 (2021).

[35] Mekatel E.H., Trari M., Nibou D., Ibtissam S., Amorkrane S., Preparation and Characterization of α-Fe_2O_3 Supported Clay as Novel Photocatalyst for Hydrogen Evolution, *Int. J. Hydro. Energy*, **44(21):** 10309-10315 (2019).